# Chiral-Icosahedral ( I ) Symmetry in Ubiquitous Metallic Cluster Compounds (145A,60X): Structure and Bonding Principles

Robert Whetten, Hans-Christian Weissker, J. Jesús Pelayo, Sean M. Mullins, Xóchitl López-Lozano, Ignacio L. Garzon

# Chiral-Icosahedral (*I*)-Symmetry in Ubiquitous Metallic Cluster Compounds (*145A,60X*): Structure-Bonding Principles

*Robert L. Whetten*[1*], *Hans-Christian Weissker*[2,3], *J. Jesús Pelayo*[4], *Sean M. Mullins*[1], *Xochitl López-Lozano*[1], *and Ignacio L. Garzón*[5*]

[1]Department of Physics and Astronomy, The University of Texas at San Antonio, One UTSA Circle, San Antonio, TX 78249-0697, USA.

[2]Aix Marseille University, CNRS, CINaM UMR 7325, 13288 Marseille, France.

[3]European Theoretical Spectroscopy Facility, 91128 Palaiseau cedex, France.

[4]Escuela Superior de Apan, Universidad Autónoma del Estado de Hidalgo, Chimalpa Tlalayote, 43920 Apan, Hidalgo, México.

[5]Instituto de Física, Universidad Nacional Autónoma de México, Apartado Postal 20-364, 01000 CDMX, México

**CONSPECTUS:** There exists a special kind of perfection — in symmetry, simplicity and stability — attainable for structures generated from precisely 60 ligands (all of a single type) that protect 145 metal-atom sites. The symmetry in question is icosahedral ($I_h$), generally, and chiral icosahedral ($I$) in particular. A sixty-fold equivalence of the ligands is the smallest number to allow this kind of perfection.

Known cluster compounds that approximate this structural ideal include palladium-carbonyls, $I_h$-$Pd_{145}(CO)_{60}$, gold-thiolates, $I$-$Au_{144}(SR)_{60}$, and gold-alkynyls, $I$-$Au_{144}(C_2R)_{60}$. Many other variants are suspected. The $Pd_{145}$ compound established the basic achiral structure-type. However, the $Au_{144}$-thiolate archetype is prominent: both historically, in the abundance and ease of preparation and handling; in their proliferation in many laboratories and application areas; and ultimately in the intrinsic chirality of its geometrical structure and organization of its bonding network or connectivity. Discovered by mass spectrometry (the "30-kDa anomaly") in 1995, wherein it appeared as a broad single peak, as solitary & symmetrical as Mount Fuji, centered near 30-kDa (~ 150 Au atoms), provoking the analogy: Surely this phenomenon requires a unique explanation. It appears to be the Buckminsterfullerene (carbon-60) of the gold-cluster chemistry.

Herein we provide an elementary account of the unexpected discovery process, in which the $Pd_{145}$-structure played a critical role, that led to the identification and correct prediction, in 2008, of a fascinating new molecular structure-type, evidently the first of chiral icosahedral symmetry. Rigorous confirmation of this prediction occurred in early Spring (2018), when two single-crystal X-ray crystallography reports were submitted, each one distinguishing both enantiomeric structures and noting profound chirality for the surface (ligand) layer.

Our emphasis is on the structure and bonding principles, and how these have been elucidated. Our aim has been to present this story in simplest terms, consistent with an extreme simplicity of the structure itself. Because it combines intrinsic profound chirality, at several levels, with the highest possible symmetry-type (icosahedral), this may attract broader interest also from educators, especially if studied in tandem with the analysis of hypothetical hollow (shell) metallic systems that exhibit the same chirality & symmetry. Because the shortest (stiffest) bonds follow the chiral 3-way weave pattern of the traditional South-Asian football, this cultural artifact may be used to introduce chiral-icosahedral symmetry in a pleasant and memorable way. One may also appreciate easily the bonding and excitations in *I*-symmetry metallic nanostructures via the golden fullerenes, i.e. the proposed hollow $Au_{60,72}$ spheres. Beyond any aesthetic or pedagogical value, we aim that our *Account* provides a clear basis upon which others may address open questions and opportunities they present.

This *Account* can only hint at the prospects for further fundamental understanding of these compounds, as well as a widening sphere of applications (chemical, electronic, imaging). The compounds remain crucial to a wider field presently under intense development.

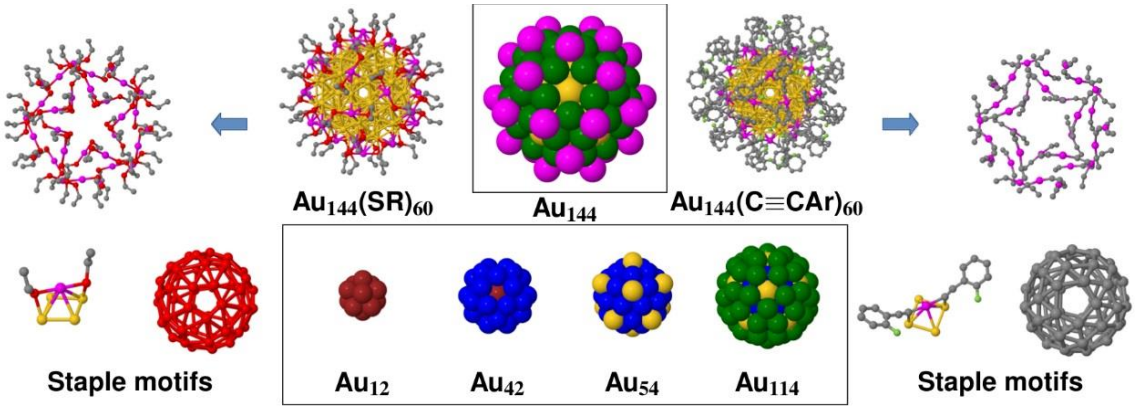

## 1. History of the *I*-(*145A,60X*)-compounds.

Are there new principles of molecular structure and bonding awaiting discovery through research on atomically precise clusters? Here, we gather evidence for structures of *chiral-icosahedral (I) symmetry* in ubiquitous noble-metal clusters comprising 145 metal-atom sites and precisely 60 anionic ligands.

In the classification of molecular structures, icosahedral symmetry ranks *highest*. It is defined by 21 axes of rotation {6 $C_5$, 10 $C_3$, 15 $C_2$} [see Fig. 1(a)]. But chirality is a case of *broken* (*lowered*) *symmetry*, reflecting non-superimposable mirror images [Fig. 1(b)]. How can a single structure integrate these elements? Earlier discussions of potential *I*-symmetry molecules describe these as *unprecedented*, as a "difficult problem in stereochemistry".[1] Then it would be so remarkable if such structures arise naturally! In the case of the abundant 145-site metallic clusters — archetypically gold-thiolate compounds *I*-$Au_{144}(SR)_{60}$ — the earlier speculations of a simple *I*-symmetry motif have been confirmed by single-crystal X-ray diffractometry .[2,3]

The structures share features with an *achiral* $I_h$-$Pd_{145}$ structure.[4] Both have concentric shells of {1@12@(30+12)@60@30} metal-atom *A*-sites. Both also have 60 bridging ligands *X*-sites, i.e. (*145A,60X*). But in key respects they differ. Not only do the $Au_{144}$ clusters offer high stability and metallic character.[5,6] They also feature a *central vacancy* and an *intrinsically chiral* surface-chemical bonding network. The locations of the coordinating atoms (*60A,60X*) resemble the achiral and chiral Archimedean (60-vertex) polyhedral forms, see Fig. 3.[7] And the shortest (strongest) bonds follow the chiral 3-way weave pattern of the traditional South-Asian football [Fig. 1(c)] .[8]

Here, we recount the discovery of the $Au_{144}$-thiolate compounds;[9] their association with the $I_h$-$Pd_{145}$ structure-type; the analytical challenge they long presented prior to a partial understanding;[10] and the recent establishment of the structure.[2,3] Theoretical advances predicted the structures to a remarkable precision, including the nature (or source) of the chiral-icosahedral (*I*)-symmetry.[11,12] Simplified pictures of electronic structure & bonding are crucial to allow all chemists to comprehend the principles that are common to a wide range of other ('atomically precise') ligand-protected noble-metal clusters, but are best exemplified in the case of highest symmetry and simplest organization.[13-15] Among the more fundamental properties predicted and observed are the electrical (electro-chemical) phenomenon of 'molecular capacitance', and the unusually discrete optical absorption spectra, as indications of metallic bonding character.[16,17] Finally, we devote special attention to the analysis of the *chirality* of (*145A,60X*) compounds: its origin, its measure (magnitude) and diverse manifestations.

**1.1 Basic Observations**. The earliest recorded encounter occurred in 1995,[18] after using a single-phase variant of the Brust-Schiffrin 2-phase method,[19] which generates larger gold-rich thiolated clusters. The mass spectrum showed a single peak, centered near 30-kDa (~ 150 Au atoms). Such result demanded strong evidence of composition, that arrived in piecemeal fashion before 2008, when the precise ligand-count was finally established. Independent assessments (elemental analysis, X-ray scattering, microscopy) indicated an Au:S ratio of ~ 2.4:1, and bulk-like metallic Au-Au bonding throughout a core of diameter ~ 16-Å, which agrees with mass 30-kDa assuming a globular shape and bulk density.[17,20] IR and NMR spectra indicated that ligand RS-groups remain intact.

**1.2 A Surprising Connection**. In early 1999, large single crystals were obtained for a compound, $Pd_{145}(CO)_{60}(PEt_3)_{30}$.[4] The $Pd_{145}$-structure revealed [Fig. 2(a)] an essentially perfect icosahedral symmetry: concentric shells of 1@12@{30+12}@60 equivalent metal-atom sites in its $Pd_{115}$ core, plus 30 external Pd atoms coordinated to the $R_3P$: ligands. The carbonyl (CO) groups bridge among the shell of 60 Pd atoms.

The relevance of this wondrous $Pd_{145}(CO)_{60}(PEt_3)_{30}$ cluster to the (Au,SR) systems was unclear: Clusters of Pd (group 10, closed-shell $4d^{10}5s^0$) and Au (group 11, $5d^{10}6s^1$) are quite distinct, as are their respective coordination chemistries with carbonyl (:C=O) and thiolate (-SR, anionic) ligands.[21] But the $Pd_{145}$ crystallographic coordinates yielded an astoundingly good match (after dilation to account for the larger size of the Au atoms) to the measured X-ray scattering function of the ~ 30-kDa gold compound. All previous structural models had failed this simple test, the hypothesis emerged that the mystery compound contained an icosahedral 145 metal-site structure, denoted "$I_h$-$Au_{145}$".

**1.3 Analytical Challenge.** The serious problem was that they long remained refractory to precise determination of composition and structure. During this period ('97 - '06), many labs prepared and used ~ 30-kDa substances, frequently adopting their own nomenclature, based on diverging imprecise estimates of the ligand and metal-atom number. (Similar confusion affected analysis of smaller clusters, during this period.)[22] This uncertainty hardly affected practical work directed toward applications of the substances, which proliferated because they are stable in air, moisture, light, and thermally; and thus, are facile to prepare, purify and handle.

The analytical problem lay in the deficiencies of then-extant methods for solving anything as complex as "$Au_{145}(SR)_{60}$", notwithstanding the prior structure determination of $Pd_{145}(CO)_{60}$. As

a result, during 1998-2005 the major advances came on smaller homologs, adapting the methods of molecular biology. By 2005, the high-resolution ESI-MS work of clusters separated by gel electrophoresis[23] established precise compositions for several smaller gold-thiolate compounds, e.g. $Au_{25}SG_{18}$, where GSH is the tripeptide glutathione.

**1.4 Crowding relieved by chirality**. An early objection to the "$Au_{145}(SR)_{60}$" structure was that there is simply too little space (too much steric crowding) for the 60 alkyl-thiolates to fit around the globular $Au_{115}$ core of icosahedral *($I_h$)* symmetry. But a reduction from full icosahedral ($I_h$) to chiral-icosahedral (*I*) symmetry liberates sufficient space to introduce four more ligands, e.g. an increase from 56 to 60. [To see this, compare the two closely-related Archimedean polyhedra, (3.4.5.4) and (3.3.3.3.5*), shown in Fig. 3.[7] Here 60 vertices represent 60 S-atoms, or α-methylene-groups (-$CH_2$-), or both. With a fixed inter-group distance as a unit, the surface area required by 60 vertices (ligands) is 55.28 units for the chiral structure, vs. 59.30 for the achiral, an increase +7.3%.] This was the first indication that chirality may be intrinsic to these substances.

Soon after came the news (in mid-2007) that the Stanford biophysical group[13] had succeeded to solve the crystal structure of a slightly smaller compound, namely (*102,44*), where R = pMBA. By determining the location of all heavy atoms (Au, S, C, O), one finally achieved a detailed picture of how the surface chemical bond is compatible with a large (79-atom) core structure that appears in many respects like bulk metallic gold.[23]

**1.5 Composition (*144,60*) Established**. Before a complete structure-model could be tested, one final piece of the puzzle needed to fall into place. In 2008, Chaki et al.[10] reported electrospray mass spectrometry (ESI-MS) of a series of the "30-kDa" Au-alkane-thiolate samples. Using the strongest peaks only, the consistent answer was (*144,59*), i.e. 144 Au atoms and 59 thiolate ligands,

the conclusion reported. However, using the less-intense peaks at slightly higher masses, one arrives at the numbers (*144,60*), in agreement with the $Pd_{145}(CO)_{60}$-based expectation that 60 ligands were required to protect the icosahedral core structure.[10] Subsequent work confirmed the (*144,60*) composition.[24,25]

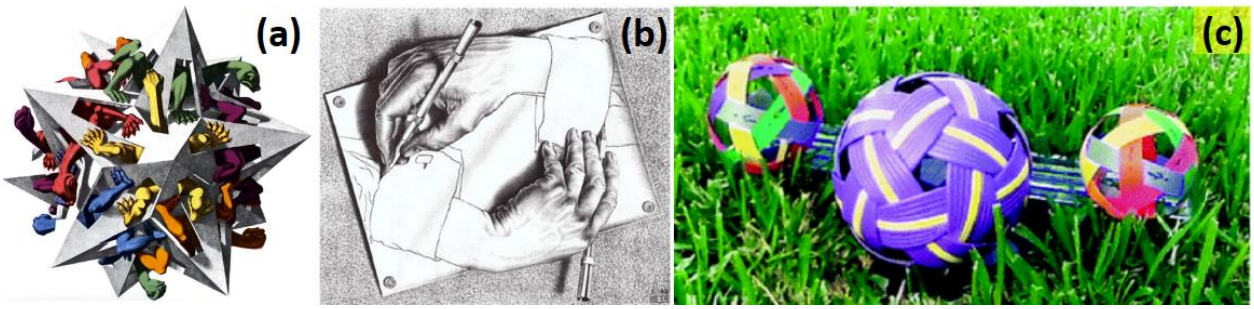


**Figure 1:** (a) Escher's rendition of icosahedral symmetry; (b) Escher's "Drawing hands" represents non-superimposable mirror-images, or enantiomeric forms; (c) the traditional South-Asian football combines these elements; it is centered between two enantiomeric models thereof.

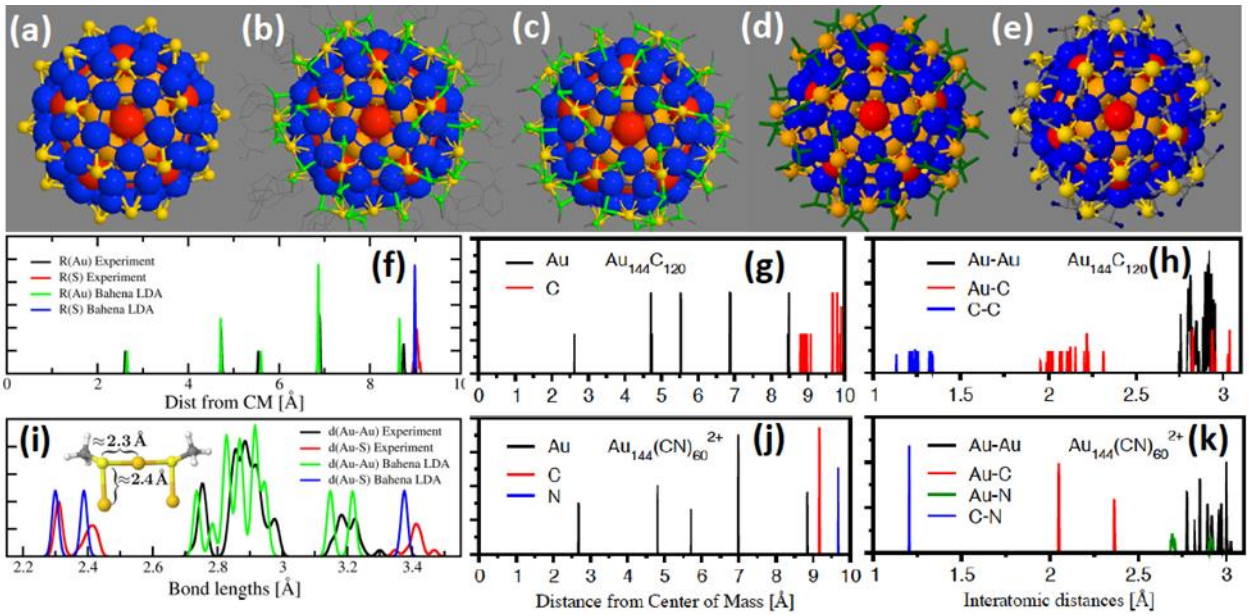

**Figure 2:** (a) $I_h$-$Pd_{145}$ experimental structure;[4] (b) $Au_{144}(SCH_2Ph)_{60}$ experimental structure;[2] (c) *I*-$Au_{144}(SCH_3)_{60}$ theory-predicted structure;[34] (d) $Au_{144}$(phenyl-alkynyl)$_{60}$ experimental structure;[3] (e) *I*-$Au_{144}(CN)_{60}$ theory-predicted structure. (C grey, N navy).[8] Metal atoms on $C_5$ axes (*red*); on $C_2$ axes (inner *orange*, outer *gold*); not on rotational axes (*blue*). At lower left, the distribution of atoms from the center of mass (f) and from nearest neighbors (i), for the experimental vs. predicted $Au_{144}$(thiolate)$_{60}$ compounds. The inset (i) depicts the all-trans configuration of the staple-motif. Lower parts middle (g,j) and right (h,k) are similar, but for the all-alkynyl $Au_{144}$ structure vs. the predicted all-cyano $Au_{144}$ structure.

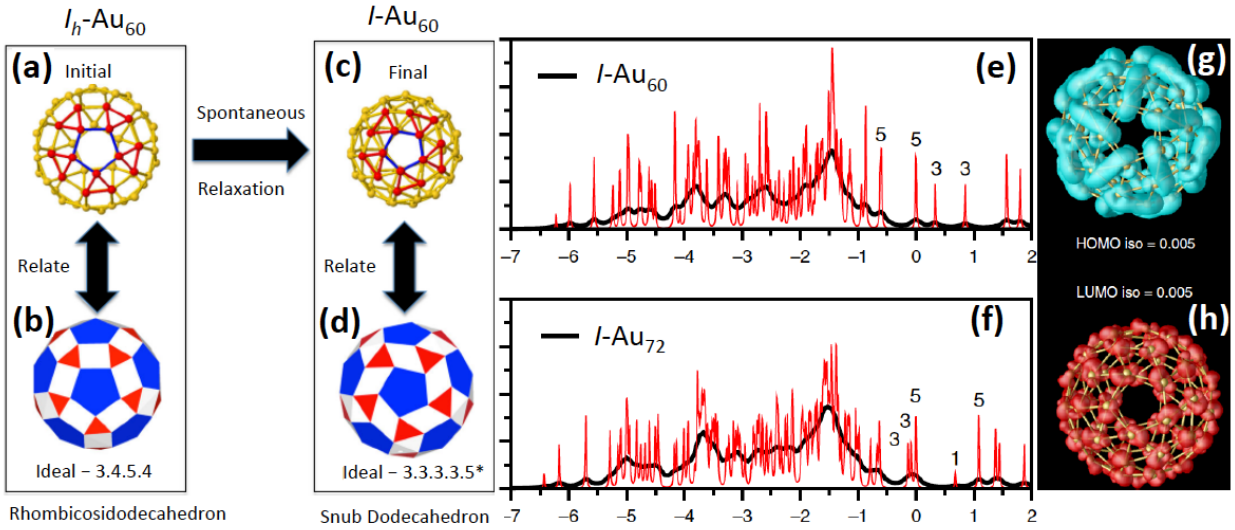


**Figure 3**: (a-d) Representation of the achiral-chiral transition, or symmetry-breaking, illustrated by the transition between the two relevant polyhedra (lower left, b-d). Electronic structure (orbital energy levels, center panel, e-f) of chiral gold shells.) [All diagrams are adapted from the recent report of Mullins et al.[7]]

## 2. Structure and Bonding in the *I*-(*145A,60X*) compounds.

**2.1 First Complete Model**. By combining the $Pd_{145}$-structure with the composition (*144,60*) and the 'staple-motif' mode of ligand coordination, one could construct a realistic and complete model of the type *I-*$Au_{145}(SR)_{60}$ and then refine it by *state of the art* DFT-based electronic-structure calculations.[11] By starting from the available $Pd_{145}$ coordinate-set, 30 pairs of bridging thiolates were inserted, colinear with an external Au(I) site and each one linked to one (of 60) surface Au-atoms. The staple motifs span diagonally the rectangular edges of the $I_h$-$Au_{115}$ grand core. The construction process further confirmed the following extraordinary (non-obvious) fact: *There exists only one way* (or two, if counting enantiomers) *to accomplish this construction. The structure is intrinsically chiral structure,* not only for the steric reasons (above), but also as demanded by the coordination of the Au(I)-thiolate staple-motifs**.** In refining the structure at a low level, it was found that the structure is more stable (less strained) minus the central atom, i.e. *one of the 145 sites remains vacant*. The model was then optimized at the highest level then feasible and reported along with many predictions.[11] During the next decade, this "Standard Model" accounts for numerous experimental results, on $A_{144\text{-}5}X_{60}$ systems (A = Au, Ag, Cu, Pd; X = thiolate variants),[26] a few mentioned below. [27,28,29]

**2.2 *I*-Symmetrization**. In 2012, the compound $Au_{144}(SCH_2CH_2Ph)_{60}$ was used as a 'target' to demonstrate rapid scanning single-molecule structure determination by selected area electron diffraction.[30] This provided motivation to complete the 'symmetrization' of the Standard Model,[11] a task initiated by Tlahuice et al.[8] and reported by Bahena et al.[30] The symmetrized structure was then reduced, by iso-electronic substitution [Fig. 2(h)], to a form manageable for detailed analysis of the structure-bonding principles.[8] Two key lessons extracted were (i) the *exactness of the I-symmetry*, whenever the charge-state permits a closed electronic shell (Fig. 4); and (ii) the

identification of a set of (60) exceptionally short Au-Au radial bonds that complete simple weave pattern [Fig. 1(c)]. Low-temperature EXAFS results subsequently confirmed both the short bonds and weave pattern, as well as the high 'bond stiffness' (mechanical rigidity).[27]

One could further refine the symmetrized structures, for more realistic ligands, in the various charge states (and alloying), without doing too much violence to its precepts. This subsequent work — led by Weissker et al.,[29,34] in parallel to improvements by Fortunelli et al.[31] and by Malola et al.[32] — advanced the understanding and confidence in the "Standard Model".[33]

**2.3 Totally Determined Structures and Implications**. To represent the class of *I*-$Au_{144}X_{60}$ compound, chemists demand rigorously to see at least one case of total-structure determination by single-crystal X-ray crystallography. In early Spring (2018), two such reports were submitted to journals.[2,3] Each distinguished both enantiomeric structures and noted profound chirality for the surface (ligand) layer.

The abundant detail provided by such crystallographic datasets provides rich material for comparison to predictions of theoretical models, and thus to stimulate further refinements. These are essential steps toward the ultimate goals, namely: (i) to achieve a fundamental understanding commensurate to the broader significance of the material-in-practice; (ii) to provide guidance to future high-level experimental work that confirms and complements such theoretical comprehension; and (iii) to assure those who prefer simply to use such compounds that the fundamentals are soundly understood.

**2.4 Geometrical and Electronic Structure Comparison.** A comparison of the experimental structure with the theoretical prediction is shown in Figs. 2(b, c) for the case R = $CH_2Ph$, i.e. benzyl-thiolate.[2,34] We optimized this model using the LDA functional as it was done for a cluster

of similar size, $Au_{146}(pMBA)_{57}$.[35] The connectivity between experimental and theoretical structures is the same, as is the orientation of the staples. This is a striking confirmation of the fully symmetrical structure,[29] with profound consequences for the electronic and optical properties.[29]

Expressive of the high symmetry are the narrow bond-length distributions shown in Fig. 2(h, i, k*)*. Around the central vacancy, coinciding with the center of mass, shells of {12; 30 + 12; 60; 30} symmetry-equivalent gold atoms are clearly seen. Spectacular agreement is likewise seen for the interatomic distances.

**2.5 The physical properties of the $Au_{144}$ compound** stand out amid the monolayer-protected clusters. For instance, its absorption spectra are much more structured than those of smaller or larger gold-thiolate compounds, as clearly shown in the series of absorption spectra of thiolate-protected clusters.[28,29] Figure 3. shows a comparison with the DOS of the less symmetrical "Lopez-Acevedo" structure.[34] [Here, we call "Lopez-Acevedo structure" the model that reported first the correct connectivity but lower symmetry due to cis orientation of several staple motifs[11] and "Bahena structure" refers to the symmetrized model.[29,30,34]]

Due to high symmetry, the frontier orbitals of the globular cluster follow the super-atom-complex model (SAC).[33] Angular-momentum projection shows (Fig. 4a) that states around the Fermi energy have clear angular-momentum (L) character. However, for the selected charge-state (level filling) there is only a very small HOMO-LUMO gap. Figure 4(b) shows the structured spectrum of the $Au_{144}(CN)_{60}$ model selected to compare with the all-alkynyl $Au_{144}$ cluster crystallized.

**2.6 Optical Spectra Sensitivity to Structure and Symmetry.** Low-temperature absorption spectra of $Au_{144}$ compounds show rich, individually peaked spectral features in the visible and near-infrared regions, much more so than any similar-sized system.[28,29] The spectral information

relates closely to the electronic structure, making $Au_{144}$ a convenient system to study the transition from molecular spectra in small, molecule-like clusters to larger, truly metallic nanoparticles with smooth electronic bands and smooth spectra. The plasmonic resonance starts to develop in this size range and is visible at a size of about 300 gold atoms.[32]

Figure 5 compares spectra calculated from two structures shown in Fig. 2(b,c), i.e. the one obtained theoretically (R = methyl group, fully symmetrized) versus the crystallographically determined coordinates (R = benzyl group). Clearly, at low energies, the differences remain small. Analysis of ligand and alloying (Cu for Au replacement) effects have been given elsewhere.[34,36,37]

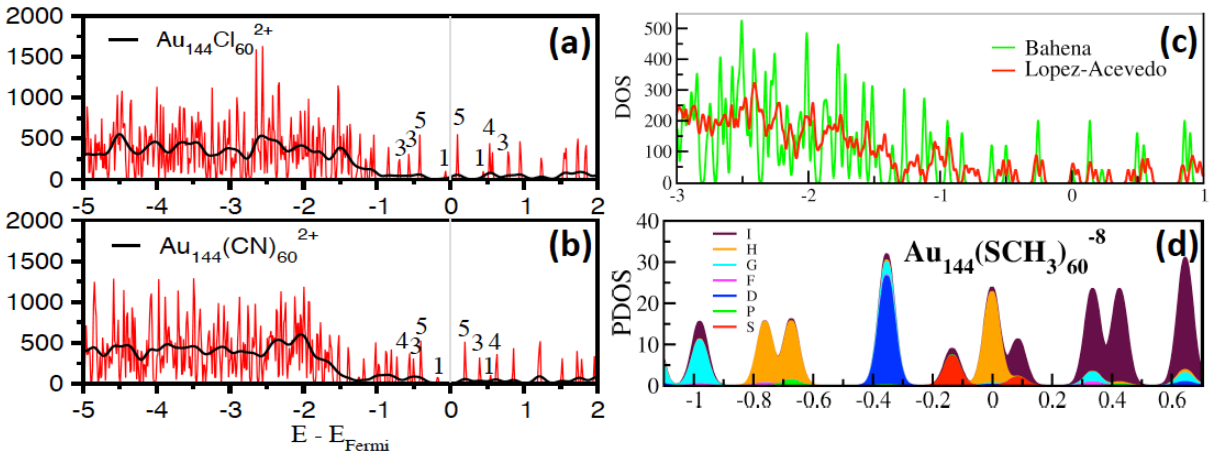


**Figure 4**: The electronic structure of the chiral-icosahedral *I*-$Au_{144}X_{60}$ compounds is represented by the orbital energy levels (horizontal axes, in eV units) and the number of orbitals (degeneracy, or density of states, *DOS*) at each energy level (vertical axis).

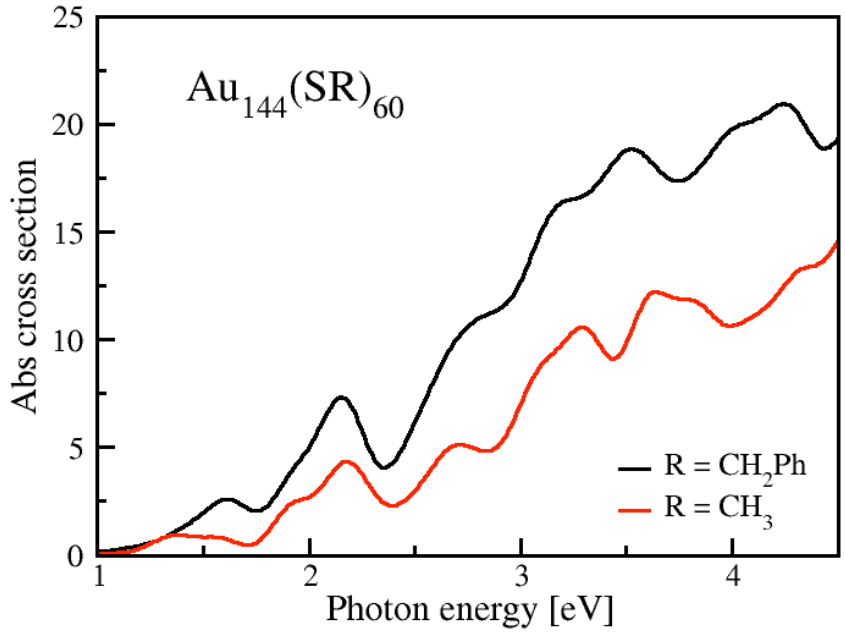


**Figure 5**: Optical absorption spectra of $Au_{144}(SR)_{60}$ compounds in the UV-vis-NIR regions. Shown is a comparison between spectra calculated by the real-time TD-DFT method assuming (red) the *I*-symmetrized structure with 60 methane-thiolate ($CH_3S$-) ligands, versus (black) the experimental structure that has 60 benzyl-thiolate ligands ($PhCH_2S$-).

### 3. Chirality in Au144 and related: Measures and Origin.

Chirality in thiolate-protected gold clusters (TPGC) $Au_n(SR)_m$ was discover around 1998-2000 by Shaaff and Whetten,[38,39] after the measurement of intense optical activity in glutathione-protected gold clusters with size < 2 nm. At the theoretical level, in 2002-2003, Garzón et al.[40,41] proposed the mechanisms to support the existence of chirality in such compounds. Later, chirality in TPGC became a hot topic in cluster science, with great progress achieved during the last 15 years, both

experimentally and theoretically (see a recent review[42] on this topic). At present, based on the divide and protect model,[43] the overall structure of $Au_n(SR)_m$ can be roughly separated into three components: the inner gold core, the intermediate Au-S interface, and the external organic ligand tail. Consequently, the chirality can be in the gold core, in the chiral arrangement of the Au-S interface motifs, or in the external organic ligand shell.[44] It also would be possible that chirality could exist simultaneously in two or three parts of the $Au_n(SR)_m$ cluster.

Chirality in the $Au_{144}(SR)_{60}$ cluster was found in the first theoretical model proposed in 2009,[11] indicating that its relaxed structure displayed a chiral icosahedral symmetry (*I*). Specifically, the polyhedral geometry of its 114-atom gold core, described as a rhombicosidodecahedron (RID), underwent a symmetry lowering from $I_h$ to *I*. This slight structural transformation is caused by the protective RS-Au-SR units capping diagonally each one of the 30 square facets of the RID, causing a distortion into the rhombic-like faces. This symmetry reduction is confirmed when analyzing the Au-Au distances at the surface of the core. Similarly to the chiral $Au_{102}(SR)_{44}$,[13] the $Au_{144}(SR)_{60}$ cluster displays a chiral arrangement of the RS-Au-SR units covering the 60-atom surface of the $Au_{114}$ core, incorporating another source of chirality onto the $Au_{144}(SR)_{60}$ cluster. Chiral icosahedral symmetry *I* was also incorporated in two subsequent theoretical models[30,34] of the $Au_{144}(SR)_{60}$ cluster, due to NMR experiments indicating that all 60 thiolates are in symmetry-equivalent configurations.[45]

To explore and gain insight into the origin and location of chirality, a geometric quantification of this property was performed using the Hausdorff chirality measure (HCM) approach.[12] The HCM analysis performed on the theoretical optimized structures of $Au_{144}(SCH_3)_{60}$[30] and $Au_{144}Cl_{60}$[8] confirmed that these clusters are chiral, with a higher contribution from the chiral arrangement of ligands than the one coming from the icosahedral core.[12] After the X-ray total structure

determination of the $Au_{144}(SCH_2Phe)_{60}$[2] and $Au_{144}(alkynyl)_{60}$[3] clusters achieved recently, it would be interesting to perform the HCM analysis using the experimental atomic positions. In this way, the theoretical model is tested, and the origin of chirality is validated through the comparison with the experimental information. Here, we present the main trends extracted from the HCM analysis performed using the recent total structure determined by x-ray crystallography.[2,3] (see Table 1 and Figs. 6 and 7).

1) $Au_{144}(SR)_{60}$: There is a very good agreement in the HCM values extracted from the theoretical[30]/ experimental[2] structures for the representative shells: $Au_{60}$ (0.019/0.021); $Au_{114}$ (0.019/0.021); $Au_{144}$ (0.015/0.016); $S_{60}$ (0.093/0.094); $Au_{30}S_{60}$ (0.090/0.091); $Au_{144}S_{60}$ (0.090/0.091) (see columns **a** and **d** in Table 1). This excellent agreement confirms that the $I_h$ to $I$ transition (chiral symmetry breaking) of the Au core induced a weak chirality, as compared with that one related with the chiral arrangement of ligands, where the 60 S atoms display a full $I$ symmetry, describing a snub dodecahedron shape. This was a conclusion mentioned in the 2015 paper,[12] however, we do not yet know the contribution of the phenyl rings to the overall chirality of the $Au_{144}(SCH_2Ph)_{60}$. Calculations of the HCM values including the 420 C atoms effect are currently under progress.

2) $Au_{144}Cl_{60}$ (see column **b** in Table 1): The HCM values for the different Au shells are slightly larger as compared to those obtained for the $Au_{144}(SCH_3)_{60}$ from Bahena et al. model[30] (column **a** of Table 1). Typical values are: $Au_{60}$ (0.029); $Au_{114}$ (0.029); $Au_{144}$ (0.230). On the other hand, the HCM for the shells involving $Cl_{60}$ are smaller as compared with the $S_{60}$ results mentioned above: $Cl_{60}$ (0.086); $Au_{30}Cl_{60}$ (0.086); $Au_{144}Cl_{60}$ (0.086). Again, in this model structure[8] it is found a weak chirality in the metal core, as compared with that one displayed by the ligand arrangement.

3) $Au_{144}C_{60}N_{60}$ (see column **c** in Table 1): The HCM values for the Au shells are intermediate between those obtained in the previous cases: $Au_{60}$ (0.025); $Au_{114}$ (0.025); $Au_{144}$ (0.019). However,

the $C_{\alpha 60}$ value is larger than that found for $S_{60}$ and $Cl_{60}$: 0.101. On the other hand, the HCM value for the $N_{60}$ shell is: 0.018, indicating almost no contribution to the overall chirality.

4) $Au_{144}(C{\equiv}CAr)_{60}$ (see column **e** in Table 1): All Au shells ($Au_{60}$, $Au_{114}$, $Au_{144}$) are achiral with HCM values smaller than $10^{-3}$. On the other hand, the $C_{\alpha 60}$ is chiral with and HCM value: 0.102. The $C_{\beta 60}$ shell is achiral with an HCM value smaller than $10^{-3}$.

In sum, for all cases investigated the chirality in the metal grand core $Au_{114}$ is weak or null. On the other hand, the shells $S_{60}$, $Cl_{60}$, $C_{\alpha 60}$ have HCM values characteristic of strong *I* symmetry: 0.086 – 0.102, indicating that chirality is mainly due to the chiral array of the protecting ligands. As was mentioned earlier, the transition from icosahedral ($I_h$) to chiral-icosahedral (*I*) symmetry appears in $Au_{144}X_{60}$ clusters compounds as the optimal solution to stabilize 30 monomeric staple motifs S-Au-S (Au-C-Au), minimizing steric effects between ligands.

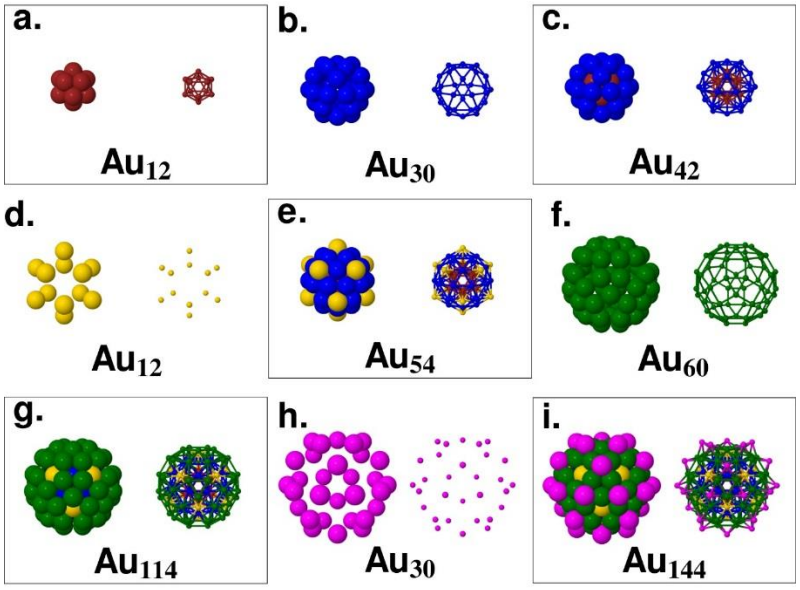


**Figure 6**. Atomic structures of the $Au_n$ shells composing the metal part ($Au_{144}$) of the $Au_{144}X_{60}$ clusters.

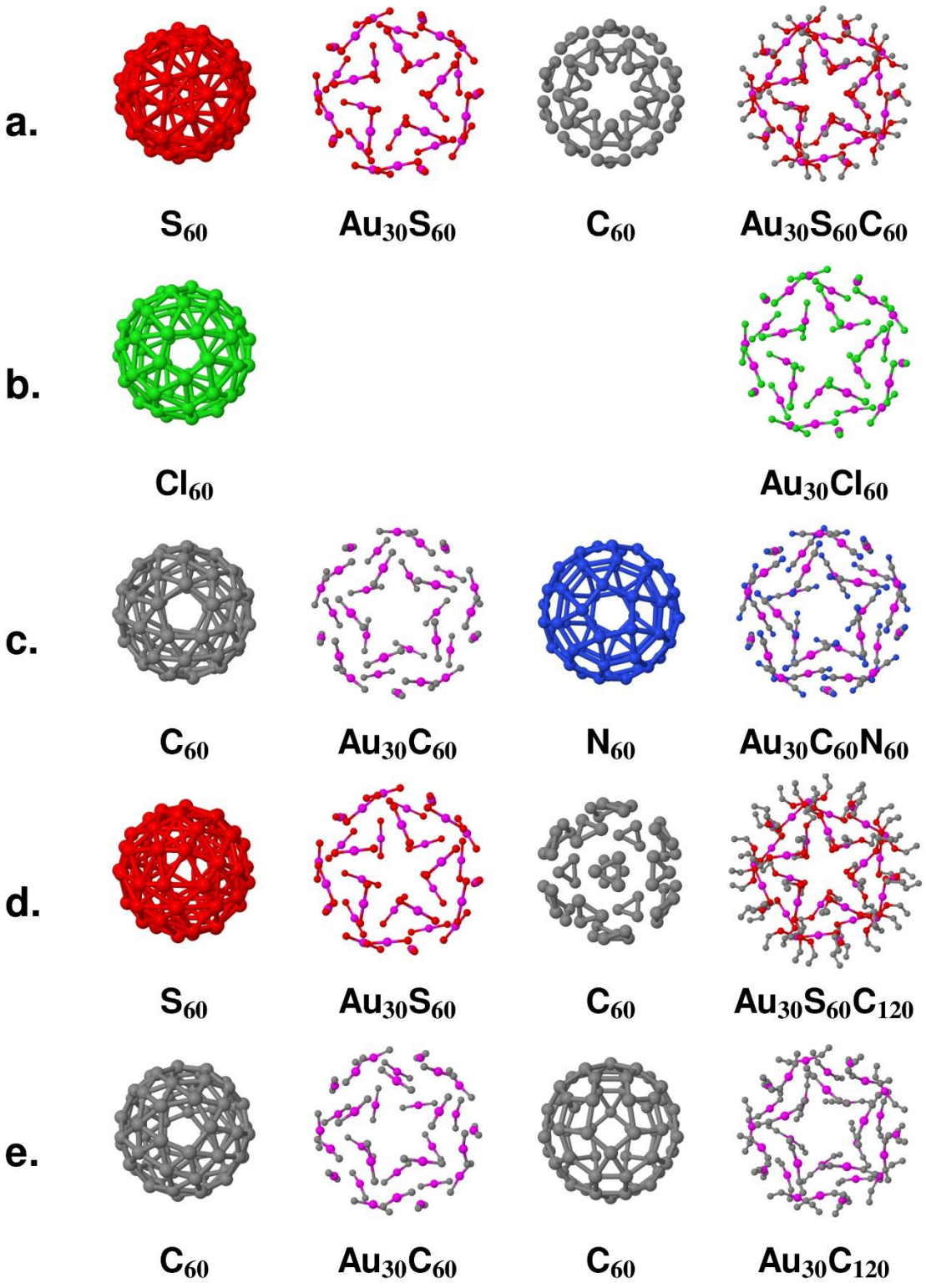


**Figure 7**. Ligand-shells of the $Au_{144}X_{60}$ clusters used for the HCM calculations. The five rows are in correspondence with the five columns shown in Table 1.

**Table 1.** Hausdorff chirality measure (HCM) values calculated using the methodology reported in Refs. 12 and 42 for different shells of the $Au_{144}X_{60}$ clusters. Cases **a** and **b** correspond to theoretical models reported in Refs. 30 and 8, respectively. Cases **d** and **e** are for the experimental X-ray structures of $Au_{144}(SR)_{60}$ ($R=CH_2Ph$) and $Au_{144}(alkynyl)_{60}$ published in Refs. 2 and 3, respectively. Cluster $Au_{144}(CN)_{60}$ (**b**) was DFT-relaxed using the methodology reported in Ref. 8. Figures 6, and 7 display the geometric structures of the all cluster shells specified in the left extrme of the Table. Point symmetry groups are also shown.

| **HCM Values and Symmetries for Protected $Au_{144}$ Clusters** | | | | | |
|---|---|---|---|---|---|
| | **a** | **b** | **c** | **d** | **E** |
| **System** | **$Au_{144}(SCH_3)_{60}$** | **$Au_{144}Cl_{60}$** | **$Au_{144}(CN)_{60}$** | **$Au_{144}(SR)_{60}$** | **$Au_{144}(C{\equiv}CAr)_{60}$** |
| $Au_{12}$ | ($I_h$) 0.000 | ($I_h$) 0.001 | ($I_h$) 0.001 | ($I_h$) 0.002 | ($I_h$) 0.000 |
| $Au_{30}$ | ($I_h$) 0.000 | ($I_h$) 0.002 | ($I_h$) 0.002 | ($I_h$) 0.003 | ($I_h$) 0.000 |
| $Au_{42}$ | ($I_h$) 0.000 | ($I_h$) 0.002 | ($I_h$) 0.002 | ($I_h$) 0.003 | ($I_h$) 0.000 |
| $Au_{12}$ | ($I_h$) 0.000 | ($I_h$) 0.003 | ($I_h$) 0.001 | ($I_h$) 0.002 | ($I_h$) 0.000 |
| $Au_{54}$ | ($I_h$) 0.000 | ($I_h$) 0.003 | ($I_h$) 0.001 | ($I_h$) 0.003 | ($I_h$) 0.000 |
| $Au_{60}$ | ($I$) 0.019 | ($I$) 0.029 | ($I$) 0.025 | ($I$) 0.021 | ($I_h$) 0.000 |
| $Au_{114}$ | ($I$) 0.019 | ($I$) 0.029 | ($I$) 0.025 | ($I$) 0.021 | ($I_h$) 0.000 |
| $Au_{30}$ | ($I_h$) 0.000 | ($I_h$) 0.002 | ($I_h$) 0.002 | ($I_h$) 0.005 | ($I_h$) 0.000 |
| $Au_{144}$ | ($I$) 0.015 | ($I$) 0.023 | ($I$) 0.019 | ($I$) 0.017 | ($D_{5d}$) 0.000 |
| $Cl_{60}$ | ------ | ($I$) 0.086 | ------ | ------ | ------ |
| $S_{60}$ | ($I$) 0.093 | ------ | ------ | ($I$) 0.094 | ------ |
| $Au_{30}C_{60}$ | ------ | ------ | ($I$) 0.095 | ------ | ($D_3$) 0.098 |
| $Au_{30}C_{120}$ | ------ | ------ | ------ | ------ | ($D_3$) 0.067 |
| $Au_{144}C_{120}$ | ------ | ------ | ------ | ------ | ($D_3$) 0.067 |
| $Au_{30}Cl_{60}$ | ------ | ($I$) 0.086 | ------ | ------ | ------ |
| $Au_{30}S_{60}$ | ($I$) 0.090 | ------ | ------ | ($I$) 0.091 | ------ |
| $Au_{144}C_{60}$ | ------ | ------ | ($I$) 0.095 | ------ | ($T$) 0.098 |
| $Au_{144}Cl_{60}$ | ------ | ($I$) 0.086 | ------ | ------ | ------ |
| $Au_{144}S_{60}$ | ($I$) 0.090 | ------ | ------ | ($T$) 0.091 | ------ |
| $C_{\alpha 60}$ | ($I$) 0.011 | ------ | ($I$) 0.101 | ------ | ($D_3$) 0.102 |
| $C_{\beta 60}$ | ------ | ------ | ------ | ------ | ($D_{3d}$) 0.000 |
| $C_{120}$ | ------ | ------ | ------ | ($D_3$) 0.075 | ($D_3$) 0.067 |
| $N_{60}$ | ------ | ------ | ($I$) 0.018 | ------ | ------ |
| $Au_{30}C_{60}N_{60}$ | ------ | ------ | ($I$) 0.050 | ------ | ------ |
| $Au_{30}S_{60}C_{60}$ | ($I$) 0.080 | ------ | ------ | ------ | ------ |
| $Au_{30}S_{60}C_{120}$ | ------ | ------ | ------ | ($T$) 0.075 | ------ |
| $Au_{144}C_{60}N_{60}$ | ------ | ------ | ($I$) 0.050 | ------ | ------ |
| $Au_{144}S_{60}C_{60}$ | ($I$) 0.080 | ------ | ------ | ------ | ------ |
| $Au_{144}S_{60}C_{120}$ | ------ | ------ | ------ | ($T$) 0.075 | ------ |

## 4. Prospectus

Prospects for future work could hardly be mentioned above, and so are presented here briefly, mainly as open questions:

**- Chirality; Enantiomer Excess; CD Spectra.** To explore chirality properties requires separate measurements on the respective enantiomers. Low temperature CD (and magnetic CD) spectra will also unravel the complex optical absorption spectrum.

**- Bonding network.** How essential is the identified weave pattern to the preferred formation of the (*145A,60X*) compounds, or their resistance to degradation? Is there an electronic origin to the unusual short-stiff metal-metal bonds, or is this a consequence of strained surface bonds?

**- The 12 other redox (charge) states.** If (as assumed) the *I*-$Au_{144}$ clusters are usually investigated in the neutral charge-state, then how do the structure-bonding properties change with charge (oxidation state) of the core? Questions concern the importance of Jahn-Teller distortions, and magnetic ordering.

**- Metal-Insulator Transition.** What is the proximity of the (*145A,60X*) compounds to a "size-induced metal-nonmetal transition", or to the emergence of the optical "plasmon" resonances. Varying the (Cu,Ag) content seems experimentally to effect such a transition, but electronic-structure theory disagrees. New approaches may be justified by the new understanding of the structure and bonding.

**- Solid-state chemistry & physics.** High-quality crystalline samples raise the possibility of making transport measurements that are not dominated by disorder, over a wide range of temperature, pressure, and field strength. Electrical transport depends critically on the thinnest

(shortest) possible ligands, and also on electronic state (charge) of the cores. The search for higher-temperature superconductors motivated the initiation of this research program.

**- Analytical chemistry; boundaries of stability.** What fraction of the many "~ 1.8- or 2-nm gold nanoparticles" already in use actually share this composition (*144,60*) and chiral-icosahedral structure-type? Stability boundaries may be set by steric constraints, e.g. aryl-thiolates form compounds (*133,52*) and (*146,57*). Or by thiolate-deficient conditions leading to competing (*130,50*) and (*137,56*) forms.

**- Applications.** We propose that the principles identified for these compounds may have immediate consequence for the related compounds actually in use. For example, it is not widely appreciated that all 60 ligands may be chemically equivalent, which has implications for derivatives obtained via ligand-exchange or tail-group reaction. A valid structure model may thus confer greater confidence on the applications-driven.

**- Testing-ground for simple models of SAMs.** The idea of "Clusters as Molecular Surfaces" was that complex problems of surface chemistry could be addressed by exploring selected cluster 'models': How best to relate the unique trans-configuration of the (*145,60*) structure surface to self-assembled monolayers, e.g. of thiolates and others on the crystalline surfaces of bulk gold electrodes, as well as to low-dimensional metallic nanostructures?

No doubt this list remains quite incomplete, but so it must remain, for the present time. As an archetypal form, the chiral-icosahedral *I*-$Au_{144}(SR)_{60}$ system has indeed served as an iconic ensign, much as Buckminsterfullerene $I_h$-$C_{60}$ earlier: it has guided and inspired the research on larger noble-metal clusters, until they reached the point of escape from the shadow of colloidal chemistry

and emerged into the bright light of molecular science, just as the objects of molecular biology (protein chemistry) had emerged some half-century earlier.

**Corresponding Author**

*E-mail: garzon@fisica.unam.mx; *E-mail: whettenz60@gmail.com

**Biographies**

**Robert L. Whetten** is Professor of Chemical Physics at the University of Texas, San Antonio since 2012. He earned his Ph. D (1984) at Cornell University and was postdoctoral fellow at Exxon's Corporate Research Labs (1984-1985). His main research interests are physical chemistry & molecular metallurgy.

**Hans-Christian Weissker** is a research scientist of CNRS in Marseille, France. His doctorate in physics is from the University of Jena, Germany (2004). He was a postdoctoral fellow at the Ecole Polytechnique in Palaiseau, France. His research today focuses on the theoretical understanding of noble-metal clusters.

**J. Jesús Pelayo** is Associate Professor at Escuela Superior de Apan – Universidad del Estado de Hidalgo, México. He obtained a Ph. D in Materials Science at *Universidad Nacional Autónoma de México* in 2016. His research focuses in theoretical and computational studies of bare and ligand-protected metal clusters.

**Sean M. Mullins** is graduate student in physics, advised by Prof. Lopez-Lozano, at the University of Texas, San Antonio. His current interests are in computational electronic structure of metallic nanostructures.

**Xóchitl López-Lozano** is Associate Professor of Physics at University of Texas, San Antonio. She earned a Ph. D. in Physics (2005) at *Benemérita Universidad de Puebla,* México, and was a postdoctoral fellow at *UNAM*, Mexico (2006). Her main research interests are in the theory of structural, electronic, and optical properties of nanomaterials.

**Ignacio L. Garzón** is a Professor of Physics at *Universidad Nacional Autónoma de México (UNAM*). He earned his Ph.D in Physics at UNAM in 1985 and was a postdoctoral at the University of California, San Diego. His current research interests are in theoretical nanoscience including the origins and analysis of chirality at the nanoscale.

**ACKNOWLEDGMENT**

Calculations were performed at the DGTIC-UNAM Supercomputing Center under Project LANCAD-UNAM-DGTIC-049. ILG thanks support from DGAPA-UNAM under Project IN108817 and Conacyt-Mexico under Project 285821. RLW acknowledges support from the Welch Foundation (AX-1857). We thank Prof. Zhikun Wu and Prof. Quan-Ming Wang for useful discussions and for providing us with useful crystallographic data of the protected $Au_{144}$ clusters.

**REFERENCES**


1. Narasimhan, S. K.; Lu, X.; Luk, Y. Chiral molecules with Polyhedral *T*, *O*, or *I* Symmetry: Theoretical Solution to a Difficult Problem in Stereochemistry. *Chirality* **2008**, *20*, 878-884.

2. Yan, N.; Xia, N.; Liao, L.; Zhu, M.; Jin, F.; Jin, R.; Wu, Z. Unravelling the Long Pursued $Au_{144}$ Structure by X-ray Crystallography. *Sci. Adv*., **2018**. DOI: 10.1126/sciadv.aat7259.

3. Lei, Z.; Li, J.-J.; Wan, X.-K.; Zhang, W.-H; Wang, Q.-M. Isolation and Total Structure Determination of an All-Alkynyl-Protected Gold Nanocluster $Au_{144}$. *Angew. Chem. Int. Ed*. **2018**, *57*, 8639-8643.

4. Tran, N. T.; Powell, D. R.; Dahl, L. F. Nanosized $Pd_{145}(CO)_x(PEt_3)_{30}$ Containing a Capped Three-Shell 145-Atom Metal-Core Geometry of Pseudo Icosahedral Symmetry. *Angew. Chem., Int. Ed.* **2000**, *39*, 4121-4125.

5. Schaaff, T. G.; Shafigullin, M. N.; Khoury, J. T.; Vezmar, I.; Whetten, R. L. Properties of a Ubiquitous 29 kDa Au:SR Cluster Compound. *J. Phys. Chem. B*, **2001**, *105*, 8785–8796.

6. Chen, S.; Ingram, R. S.; Hostetler, M. J.; Pietron, J. J.; Murray, R. W.; Schaaff, T. G.; Khoury, J. T.; Alvarez, M. M.; Whetten, R. L. Gold Nanoelectrodes of Varied Size: Transition to Molecule-Like Charging. *Science*, **1998**, *280*, 2098-2101.

7. Mullins, S.-M.; Weissker, H.-C.; Sinha-Roy, R.; Pelayo, J. J.; Garzón, I. L.; Whetten, R. L.; López-Lozano, X. Chiral Symmetry Breaking Yields an *I*–$Au_{60}$ Perfect Golden Shell of Singular Rigidity. *Nat. Comm.* **2018***, 9*, 3352(1-9).

8. Tlahuice-Flores, A.; Black, D. M.; Bach, S. B. H.; Jose-Yacaman, M.; Whetten, R. L. Structure & Bonding of the Gold-Subhalide Cluster *I*-Au144Cl60. *Phys. Chem. Chem. Phys.* **2013**, *15*, 19191-19195.

9. Whetten, R. L.; Khoury, J. T.; Alvarez,M. M.; Murthy, S.; Vezmar, I.; Wang, Z. L.; Stephens, P. W.; Cleveland, C .L.; Luedtke, W. D.; Landman, U. Nanocrystal gold molecules. *Adv. Mater.* **1996**, *8*, 428–433.

10. Chaki, N. K.; Negishi, Y.; Tsunoyama, H.; Shichibu, Y.; Tsukuda, T.; Ubiquitous 8 and 29 kDa Gold:Alkanethiolate Cluster Compounds: Mass Spectrometric Determination of Molecular Formulas and Structural Implications. *J. Am. Chem. Soc.,* **2008**, *130*, 8608-8610.

11. López-Acevedo, O.; Akola, J.; Whetten, R. L.; Grönbeck, H.; Häkkinen, H. Structure and Bonding in the Ubiquitous Icosahedral Metallic Gold Cluster $Au_{144}(SR)_{60}$. *J. Phys. Chem*. **2009**, *113*, 5035-5038.

12. Pelayo, J. J.; Whetten, R. L.; Garzón, I. L. Geometric Quantification of Chirality in Ligand-Protected Metal Clusters. *J. Phys. Chem. C* **2015**, *119*, 28666-28678.

13. Jadzinsky, P. D.; Calero, G.; Ackerson, C. J.; Bushnell, D. A.; Kornberg, R. D. Structure of a Thiol Monolayer-Protected Gold Nanoparticle at 1.1 Å Resolution. *Science* **2007**, *318*, 430-433.

14. Chakraborty, I.; Pradeep, T. Atomically Precise Clusters of Noble Metals: Emerging Link between Atoms and Nanoparticles. *Chem. Rev.* **2017**, *117*, 8208-8271.

15. Murray, R. W. Nanoelectrochemistry: Metal Nanoparticles, Nanoelectrodes, and Nanopores. *Chem. Rev.* **2008**, *108*, 2688-2720.

16. Yau, S. H.; Varnavski, O.; Goodson, T. An Ultrafast Look at Au Nanoclusters. *Acc. Chem. Res.* **2013**, *46*, 1506-1516.

17. Whetten, R. L.; Shafigullin, M. N.; Khoury, J. T.; Schaaff, T. G.; Vezmar, I.; Alvarez, M. M.; Wilkinson, A. Crystal Structures of Molecular Gold Nanocrystal Arrays. *Acc. Chem. Res.* **1999**, *32*, 397-406.

18. Whetten, R. L.; Khoury, J.T.; Alvarez, M. M.; Murthy, S.; Vezmar, I.; Wang, Z. L.; Cleveland, C.L.; Luedtke, W. D.; Landman, U. Nanocrystal Gold Molecules, in *The Chemical Physics of Fullerenes: 10 (and 5) Years Later*, edited by W. Andreoni (NATO-ASI, 1996). Varenna, Italy, p. 475-490.

19. Brust, M.; Walker, M.; Bethell, D.; Schiffrin, D. J.; Whyman, R. Synthesis of Thiol-Derivatised Gold Nanoparticles in a Two-Phase Liquid-Liquid System. *J. Chem. Soc., Chem. Commun.* **1994**, 801-802.

20. Schaaff, T. G.; Shafigullin, M. N.; Khoury, J. T.; Vezmar, I.; Whetten, R. L.; Cullen, W. G.; First, P. N.; Gutiérrez-Wing, C.; Ascensio, J.; Jose-Yacamán, M. J. Isolation of Smaller Nanocrystal Au Molecules: Robust Quantum Effects in Optical Spectra. *J. Phys. Chem. B* **1997**, *101*, 7885-7891.

21. Mednikov, E. G.; Dahl, L. F. Syntheses, Structures and Properties of Primarily Nanosized Homo/Heterometallic Palladium CO/$PR_3$-ligated Clusters. *Phil. Trans. R. Soc. A* **2010**, *368*, 1301-1332.

22. Parker, J. F.; Fields-Zinna, C. A.; Murray, R. W. The Story of a Monodisperse Gold Nanoparticle: $Au_{25}L_{18}$. *Acc. Chem. Res.* **2010**, *43*, 1289-1296.

23. Negishi, Y.; Nobusada, K.; Tsukuda, T. Glutathione-Protected Gold Clusters Revisited: Bridging the Gap between Gold(I)−Thiolate Complexes and Thiolate-Protected Gold Nanocrystals *J. Am. Chem. Soc.* **2005**, *127*, 5261-5270.

24. Fields-Zinna, C. A.; Sardar, R.; Beasley, C. A.; Murray, R. W. ESI-MS of Intrinsically Cationized Nanoparticles $[Au_{144/146}(SC_{11}H_{22}N(C_2H_5))_x(S(C_6H_{13})_y]$. *J. Am. Chem. Soc.* **2009**, *131*, 16266-16271.

25. Qian, H.; Jin, R. Controlling Nanoparticles with Atomic Precision: The Case of $Au_{144}(SCH_2CH_2Ph)_{60}$. *Nano Lett.* **2009**, *9*, 4083-4087.

26. Kumara, C.; Dass, A. $(AuAg)_{144}(SR)_{60}$ Alloy Nanomolecules. *Nanoscale*, **2011**, *3*, 3064-3067.

27. Yamazoe, S.; Takano, S.; Kurashige, W.; Yokoyama, T.; Nitta, K.; Negishi, Y.: Tsukuda, T. Hierarchy of bond stiffnesses within icosahedral-based gold clusters protected by thiolates. *Nat. Commun.* **2016**, *7*, 10414 (1-7).

28. Negishi, Y.; Nakazaki, T.; Malola, S.; Takano, S.; Niihori, Y.; Kurashige, W.; Yamazoe, S.; Tsukuda, T.; Häkkinen, H. A Critical Size for Emergence of Nonbulk Electronic and Geometric Structures in Dodecanethiolate-Protected Au Clusters. *J. Am. Chem. Soc.* **2015**, *137*, 1206-1212.

29. Weissker, H.-Ch.; Barron Escobar, H.; Thanthirige, V.D.; Kwak, K.; Lee, D.; Ramakrishna, G.; Whetten, R. L.; López-Lozano, X., Information on Quantum States Pervades the Visible Spectrum of the Ubiquitous $Au_{144}(SR)_{60}$ Gold Nanocluster. *Nat. Comm* **2014**, *5*, 3785(1-8).

30. Bahena, D.; Bhattarai, N.; Santiago, U.; Tlahuice, A.; Ponce, A.; Bach, S. B. H.; Yoon, B.; Whetten, R. L.; Landman, U.; Jose-Yacaman, M. STEM Electron Diffraction and High-Resolution Images Used in the Determination of the Crystal Structure of the $Au_{144}(SR)_{60}$ Cluster. *J. Phys. Chem. Lett.* **2013**, *4*, 975-981.

31. Barcaro, G.; Sementa, L.; Fortunelli, A.; Stener, M. Comment on "$(Au- Ag)_{144}(SR)_{60}$ Alloy Nanomolecules" by C. Kumara and A. Dass, Nanoscale, 2011, 3, 3064. *Nanoscale* **2015**, *7*, 8166-8167.

32. Malola, S.; Lehtovaara, L.; Enkovaara, J.; Häkkinen. Birth of the Localized Surface Plasmon Resonance in Monolayer-Protected Gold Nanoclusters. *ACS Nano* **2013**, *7*, 10263–10270.

33. Walter, M.; Akola, J.; Lopez-Acevedo, O.; Jadzinsky, P. D.; Calero, G.; Ackerson, C. J.; Whetten, R. L.; Grönbeck, H.; Häkkinen, H. A Unified View of Ligand-Protected Gold Clusters as Superatom Complexes. *Proc. Natl. Acad. Sci*. **2008**, *105*, 9157-9162.

34. Weissker, H.-Ch.; Lopez-Acevedo, O.; Whetten, R. L.; López-Lozano, X. Optical Spectra of the Special $Au_{144}$ Gold-Cluster Compounds: Sensitivity to Structure and Symmetry. *J. Phys. Chem. C* **2015**, *119*, 11250–11259.

35. Vergara, S.; Lukes, D. A.; Martynowycz, M. W.; Santiago, U.; Plascencia-Villa, G.; Weiss, S. C.; de la Cruz, M. J.; Black, D. M.; Alvarez, M. M.; López-Lozano, X.; Barnes, C. O.; Lin, G.; Weissker, H.-C.; Whetten, R. L.; Gonen, T.; Yacaman, M. J.; Calero, G. Micro ED Structure of $Au_{146}$(p-MBA)$_{57}$ at Subatomic Resolution Reveals a Twinned FCC Cluster. *J. Phys. Chem. Lett.* **2017**, *8*, 5523-5530.

36. Sinha-Roy, R.; López-Lozano, X.; Whetten, R. L.; García-González, P.; Weissker, H.-Ch. In Search of the Quantum-Electronic Origin of Color Change: Elucidation of the Subtle Effects of Alloying with Copper on ≈ 1.8 nm Gold Nanoclusters. *J. Phys. Chem. C* **2017**, *121*, 5753–5760.

37. López-Lozano, X.; Plascencia-Villa, G.; Calero, G.; Whetten, R. L.; Weissker. H.-Ch. Is the Largest Aqueous Gold cluster a Superatom Complex? Electronic Structure & Optical Response of the Structurally Determined $Au_{146}$(p-MBA)$_{57}$. *Nanoscale* **2017**, *9*, 18629–18634.

38. Schaaff, T. G.; Knight, G.; Shafigullin, M. N.; Borkman, R. F. Whetten, R. L. Isolation and Selected Properties of a 10.4 kDa Gold:Glutathione Cluster Compound. *J. Phys. Chem B* **1998**, *102*, 10643-10646.

39. Schaaff, T. G.; Whetten, R. L. Giant Gold-Glutathione Cluster Compounds: Intense Optical Activity in Metal-Based Transitions. *J. Phys. Chem. B* **2000**, *104*, 2630-2641.

40. Garzón, I. L.; Reyes-Nava, J. A.; Rodríguez-Hernández, J. I.; Sigal, I., Beltrán, M. R.; Michaelian K. Chirality in Bare and Passivated Gold Nanoclusters. *Physical Review B* **2002**, *66*, 073403 (1- 4).

41. Garzón, I. L.; Beltrán, M. R.; González, G.; Gutiérrez-González, I.; Michaelian, K.; Reyes-Nava, J. A.; Rodríguez-Hernández, J. I. Chirality, Defects, and Disorder in Gold Clusters. *Eur. Phys. J. D* **2003**, *24*, 105-109.

42. Pelayo, J. J.; Valencia, I.; García, A. P.; Chang, L.; López, M.; Toffoli, D.; Stener, M.; Fortunelli, A.; Garzón, I. L. Chirality in Bare and Ligand-Protected Metal Nanoclusters. *Adv. Phys. X*, **2018**, *3*, 964-997.

43. Häkkinen, H.; Walter, M.; Grönbeck, H. Divide and Protect: Capping Gold Nanoclusters with Molecular Gold-Thiolate Rings. *J. Phys. Chem. B* **2006**, *110*, 9927-9931.

44. Zeng, C.; Jin, R. Chiral Gold Nanoclusters: Atomic Level Origins of Chirality. *Chem. Asian J.* **2017**, *12*, 1839-1850.

45. Wong, O. A.; Heinecke, C. L.; Simone, A. R.; Whetten, R. L.; Ackerson, C. J. Ligand-Symmetry-Equivalence on Thiolate Protected Gold Nanoclusters determined by NMR Spectroscopy. *Nanoscale* **2012**, *4*, 4099-4102.